Conf-910646--3

γ

ION IMPLANTATION EFFECTS IN CRYSTALLINE QUARTZ

G. W. Arnold
Ion-Solid Interactions Division 1111
Sandia National Laboratories
Albuquerque, NM 87185 USA

SAND--91-0863C
DE91 016192
AUG 0 5 1991

ABSTRACT

Cantilever beam measurements of the stress induced in crystalline quartz by implantation of 150 keV Ar and/or 250 keV He have shown that the data scale with energy into collisional processes. The damage state induced by the Ar implants does not lend itself to efficient utilization of the electronic component of subsequent He implantation in producing further disorder. The damage depth has been measured (optically) for a number of ions (1×10^{16} 250 keV/cm^2) and has been found to vary (relative to TRIM values) from about $0.63R_p$ for He to about $1.84R_p$ for Xe. RBS measurements of range for Ar to Au give values in fair agreement with the optical values. The ratio of the measured (optical) ranges to the predicted (TRIM) ranges, when plotted as a function of collisional energy deposition, indicates that extended damage (beyond ion range) occurs for deposition energies >~1×10^{22} keV/cm^3. The damage persists even after 900°C anneals. The effects of ion-induced stress may be an important factor in the establishment of the extended damage state.

1. INTRODUCTION

Our understanding of the ion-induced damage processes in crystalline quartz is due, in large measure, to the extensive work of the Jena (Germany) group [1-5]. Of particular interest are the observations [1] utilizing Rutherford backscattering-channeling (RBS-C) which showed that lattice damage induced by 150 keV Ar, at fluence levels below that necessary to reach the random disorder state, produced a condition in which further disorder could be generated by the largely electronic energy deposition from a 1.4 MeV He implantation. He implantation alone did not produce RBS-C disorder. It was also shown that Ar implantation at fluence levels greater than that required for random disorder resulted in a proportionally deeper development of the damage state.

We have utilized cantilever-beam [6-8] measurements of ion-induced surface stress in the present investigation as a means of further studying the effects of energy deposition and partition in crystalline quartz. We have, in addition, made measurements of the effective range over which implanted ions (1×10^{16} 250 keV; H-Au) alter the properties of quartz as measured by the interference fringes produced in transmission of light and have monitored the structural damage (IR reflection measurements).

Our cantilever-beam results show equal effectiveness of 150 keV Ar and 250 keV He in producing lateral surface stress when plotted against energy into collisional processes. The ranges over which ions produce interference fringes increase with the mass of the ion and vary from $0.64R_p$ (He) to $1.84R_p$ (Xe). The RBS range measurements for Ar-Au are in fair agreement with the optical values and lead to the establishment of a threshold deposition energy for production of extended damage. These results are consonant with those of the Jena group as respecting the increased damage range with increasing fluence and the apparent differences between our cantilever-beam measurements and the RBS-C measurements are viewed as an indication of the greater sensitivity of the RBS-C measurements to the off-lattice site movements of SiO_4 groups upon bond-breakage by ionization.

2. EXPERIMENTAL

Cantilever-beam samples were prepared (1.2 x .2 x .02 cm) from the slow-growth Z-sectors of Y-bar synthetic quartz [9] and an Al film (150) was deposited on both major surfaces of the beams. The cantilever-beam apparatus has been previously described [8]. Implantations for these samples and for the samples used for the interference-fringe measurements of range were made either with an Accelerators, Inc. implanter or with a High Voltage Europa machine. In the present experiments, 250 keV He was used to provide electronic energy deposition throughout the Ar implanted damage region. This is a major difference between our conditions and those of the Jena group, who used 1.4 MeV He for this purpose, but should be significant primarily in terms of electronic energy deposition rates since both He ions come to rest well beyond the Ar range.

The optical measurements of range were made with a Varian 2300 spectrometer. The infrared reflection measurements were made with a Nicolet FTIR instrument. The RBS range measurements were made using a 2.8 MeV He beam and standard geometry and detection techniques.

3. RESULTS AND DISCUSSION

The surface compressive stress resulting from 150 keV Ar implantation is shown in Fig. 1 as a function of ion fluence. The results for 250 keV He implantation alone and following an Ar implantation to a fluence level of 2 x 10^{13} 150 keV Ar/cm^2 are shown in Fig. 2. Except for small differences at low fluence levels, the data of Fig. 2 indicate that the prior Ar implant does not effectively alter the results obtained for He implantation alone. Figure 3 compares the results for He and Ar implants as a function of ion fluence. The differences in stress levels are due to the differences in ranges. This data presentation is to be compared with that of Fig. 4 in which stress is plotted as a function of energy into collisional processes. The data of Fig. 4 clearly show that the maximum yield stress is attained for the same collisional energy deposition for both He and Ar implantations. Furthermore, this stress level is reached at about 2 x 10^{20} keV/cm^3, i.e., at the same critical energy deposition value which has been found to produce the maximum change in a number of physical properties altered by ion-implantation in silica glasses [10,11] and quartz [1].

The data of Fig. 2 are to be contrasted with the RBS-C data of the Jena group [1] who found that the same 2 x 10^{13} 150 keV Ar implant followed by a 1.4 MeV He implant produced levels of damage greater than that produced by the Ar implant alone and that 1.4 MeV He implantation alone did not result in the production of RBS disorder. The RBS-C method will detect off-site displacements in the crystal lattice of 0.2 or greater. Bond-breaking by electronic energy deposition in an already strained lattice can be expected to result in a relaxation of the separated partners away from each other and a resultant shift in lattice positions. The RBS-C technique can be expected to see these small movements and register them as contributing to the measured disorder but these movements are not, apparently, discerned by the cantilever-beam technique.

The change in density of quartz, from 2.65 to about 2.24, as a consequence of amorphization, produces a corresponding change in refractive index. This change in index allows interference fringes to be readily measured in transmission in a spectrophotometer and a consequent measurement of the effective damage depth. Table 1 lists the ions (all at 250 keV and 1 x 10^{16}/cm^2), the measured damage depths (optical and RBS), and the TRIM (R_p) ranges [12]. The ratio (R_{opt}/R_{TRIM}) varies from 0.64 for He to 1.84 for Xe. The Jena group also measured greater than predicted values at fluence levels greater than those required to reach random levels with Ar implants. In Fig. 5 is plotted the ratio (R_{opt}/R_{TRIM}) values from Table 1 as a function of collisional energy deposition for the various 250 keV ions. There is seen to be a threshold energy of about 1 x 10^{22} keV/cm^3 above which the effective, or extended, damage depth begins to markedly exceed the TRIM values. This is the same result found [13] for a variety of experimental results for silicate glasses. It has been speculated that the effect may be due, in part, to the effects of implantation-induced stress [13]. There may also be effects due to the increased knock-on momentum as the ion mass increases.

Figure 6 shows the infra-red reflectance spectra for a sample implanted with Ar at the indicated energy and fluence compared to the unimplanted side of the sample. The shift to lower wavenumber of the Si-O-Si stretch lattice mode and the diminished intensity as well as the other features are typical of ion-implanted quartz and have been noted elsewhere [13, 14]. Figure 7 shows that these structural damage features are not completely annealed out even after a 1 hr 900°C anneal. The corresponding interference fringe pattern also persists after this anneal. The damage features (not shown) due to charge-trapping (E'- and B_2-centers) anneal out at temperatures near 600°C.

4. CONCLUSIONS

We find that:

1.) The lateral compressive surface stress generated by 150 keV Ar and for 250 keV He implantation scales with energy into collisional processes.

2.) Prior damage (2×10^{13} 150 keV Ar) has negligible effect on the damage induced by subsequent 250 keV He implantation.

3.) Separate experiments on range determinations for various 1×10^{16} 250 keV ions (by interference-fringe measurements) show increases over theoretical ranges by as much as 1.84. RBS range measurements were also made and are in fair agreement with the optical range values. The ratio of range measured optically to TRIM ranges, when plotted against collisional energy, shows that an extended damage threshold exists at about 1×10^{22} keV/cm^3, in agreement with detailed studies on silicate glasses [13].

4.) The structural damage (as measured by IR reflection) due to ion implantation persists after anneals of 900°C for 1 hr.

5. ACKNOWLEDGEMENTS

The author gratefully acknowledges the assistance of K.G. Minor and N.D. Wing in various phases of these experiments. This work was supported by the U.S. Department of Energy under Contract DE-AC04-76-DP00789.

REFERENCES

[1] H. Fischer, G. Gotz, and H. Karge, Phys. Stat. Sol. (a)76, 249 (1983).

[2] H. Fischer, G. Gotz, and H. Karge, Phys Stat. Sol. (a)76, 493, (1983).

[3] H. Karge and R. Prager, Exper. Tech. Phys. 24, 87 (1976).

[4] U. Katenkamp, H. Karge, and R. Prager, Rad. Effects 48, 31 (1980).

[5] G. Gotz, in Ion Beam Modification of Insulators, P. Mazzoldi and G.W. Arnold (Eds.), (Elsevier, 1987), p. 412.

[6] E.P. EerNisse, Appl. Phys. Lett. 18, 581 (1971).

[7] E.P. EerNisse, J. Appl. Phys. 45, 167 (1974).

[8] C.B. Norris and E.P. EerNisse, Rev. Sci. Instrum. 54, 552 (1983).

[9] G.W. Arnold, Phys. Chem. Solids 13, 306 (1960).

[10] G.W. Arnold, Rad. Effects 65, 17 (1982).

[11] G.W. Arnold and P. Mazzoldi, in Ion Beam Modification of Insulators, P. Mazzoldi and G.W. Arnold (Eds.), (Elsevier, 1987), p. 195.

[12] J.F. Ziegler, J.P. Biersack, and U. Littmark, The Stoppng Power of Ions in Solids, (Pergamon, New York, 1985).

[13] G.W. Arnold, G. Battaglin, A. Boscolo-Boscoletto, F. Caccavale, G. De Marchi, P. Mazzoldi, and A. Miotello, (these Proceedings).

[14] G.W. Arnold, in The Physics of SiO_2 and its Interfaces, S.T. Pantelides (Ed.), (Pergamon, 1978), p. 278.

TABLE 1

Range measurements (optical and RBS) for 1 x 10^{16} 250 keV ions/cm^2 on crystalline quartz compared to theoretical values of R_p (TRIM).

Ion	Range (opt) ( )	Range (RBS) ( )	Range (TRIM) ( )	R(opt.)/R(TRIM)
H	19880	---	19200	1.04
He	6733	---	10683	0.63
O	3434	---	4110	0.84
Ne	3513	---	3888	0.90
Ar	2274	2500	2024	1.12
Cu	2034	2400	1550	1.31
Kr	1844	2300	1262	1.46
Xe	1486	1580	808	1.84
Au	1247	1850	729	1.71

FIGURE CAPTIONS

Fig. 1 Implantation stress (dynes/cm) vs 150 keV Ar fluence (ions/cm^2) incident on crystalline quartz.

Fig. 2 Implantation stress (dynes/cm) vs 250 keV He fluence (ions/cm^2) for (a) 250 keV He only and (b) for 250 kev He following an implantation of 2 x 10^{13} 150 keV Ar/cm^2.

Fig. 3 Implantation stress (dynes/cm) vs ion fluence (ions/cm^2) for a sample implanted with 250 keV He and for a sample implanted with 150 keV Ar.

Fig. 4 Implantation stress (dynes/cm) vs energy into atomic collisions (keV/cm^3) for the 250 keV He and for the 150 keV Ar implanted samples of Fig. 3.

Fig. 5 The values of R_{opt}/R_{TRIM} (from Table I) vs energy into collisional processes for the same 1 x 10^{16} 250 keV ions/cm^2.

Fig. 6 Infrared reflectance vs wavenumber (cm^{-1}) for crystalline quartz implanted with 3.52 x 10^{16} 200 keV Ar^{++}/cm^2 compared to the unimplanted side of the sample.

Fig. 7 Infrared reflectance vs wavenumber (cm^{-1}) for the sample of Fig. 5 after implantation and after anneals at 600°C and 900°C.

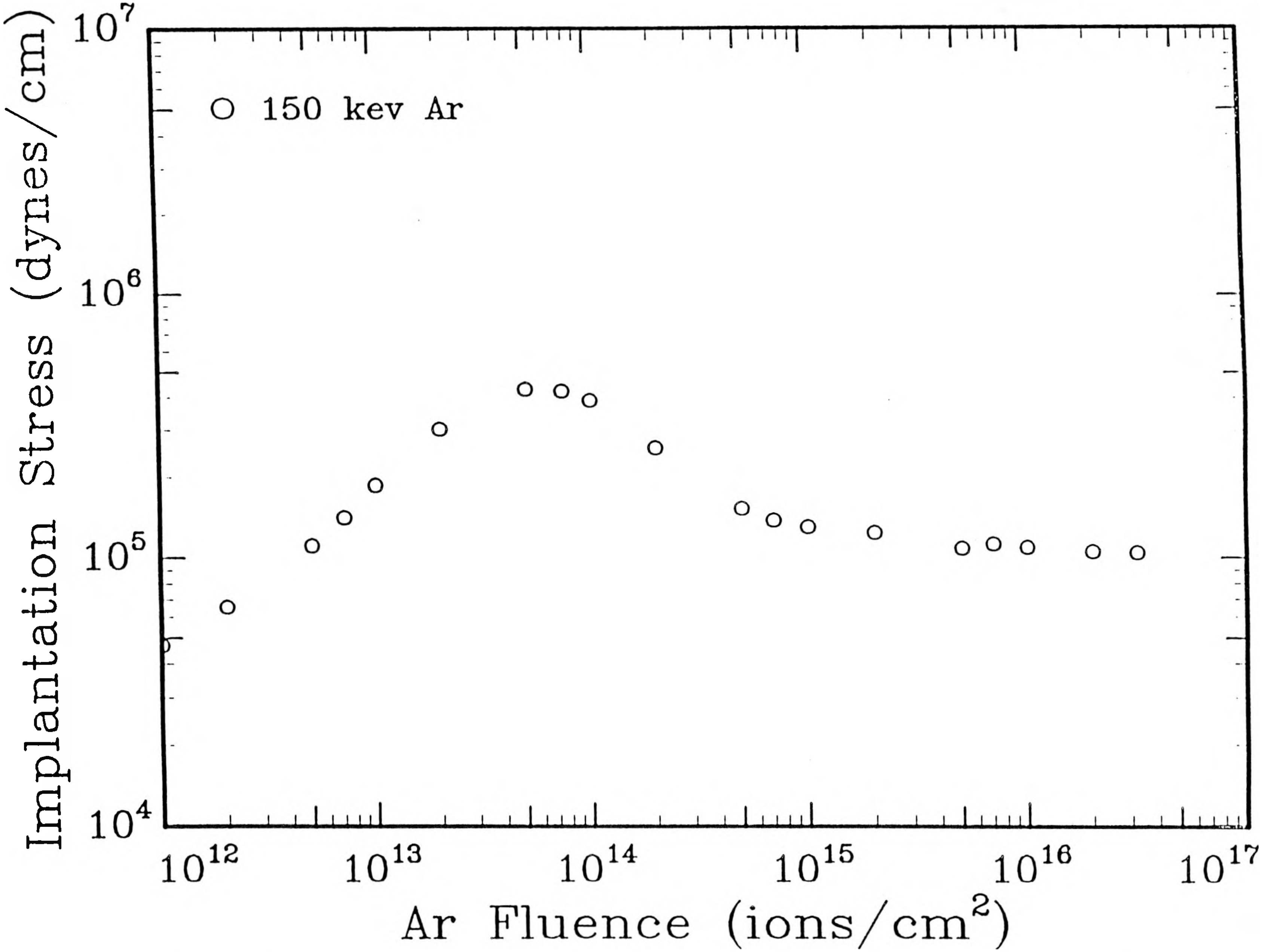
Implantation Stress (dyne/cm)
○ 150 kev Ar
10^7
10^6
10^5
10^4
10^12
10^13
10^14
10^15
10^16
10^17
Ar Fluence (ions/cm^2)

Figure 1

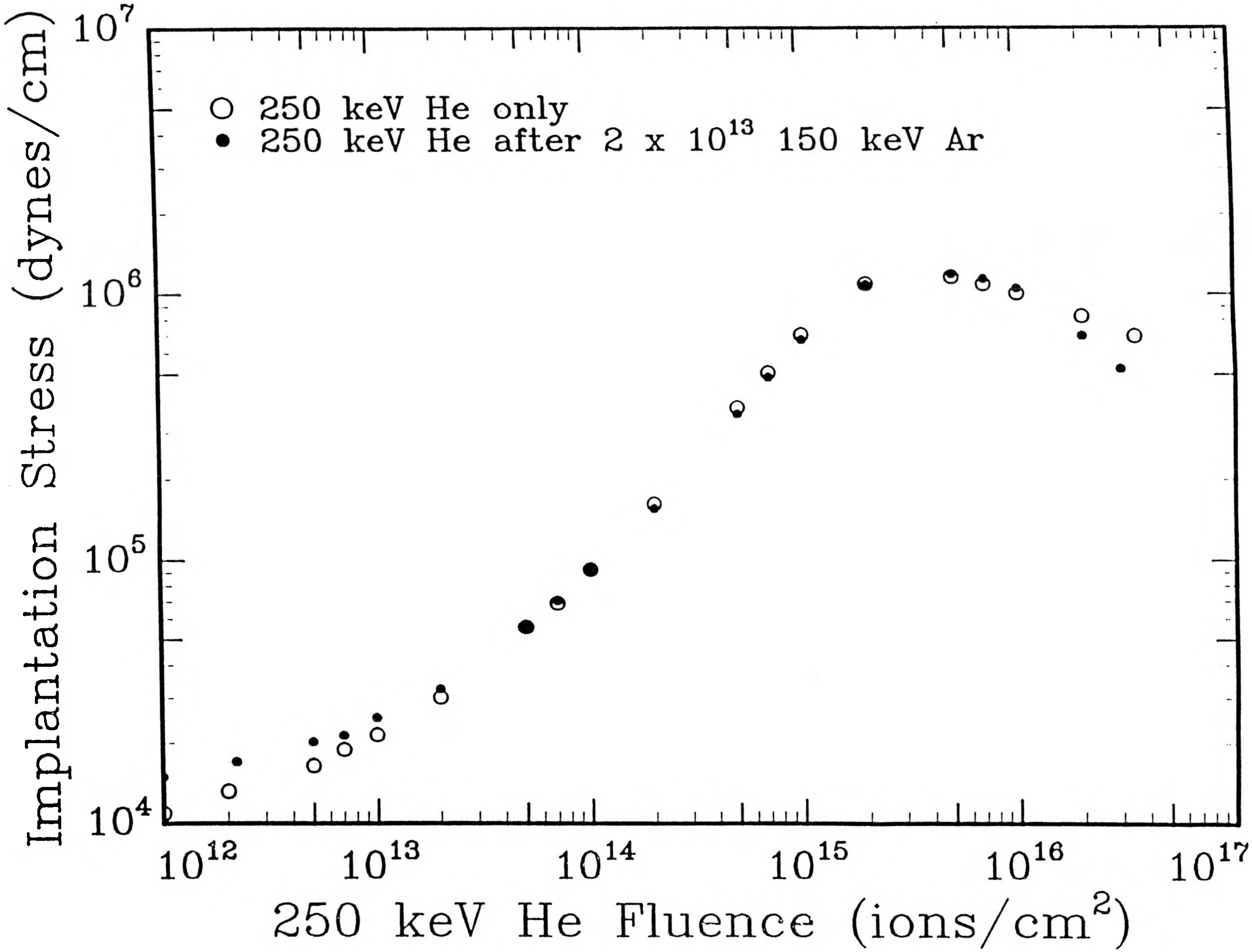

○ 250 keV He only
● 250 keV He after 2 x 10^13 150 keV Ar
Implantation Stress (dynes/cm)
10^7
10^6
10^5
10^4
10^12
10^13
10^14
10^15
10^16
10^17
250 keV He Fluence (ions/cm^2)

Figure 2

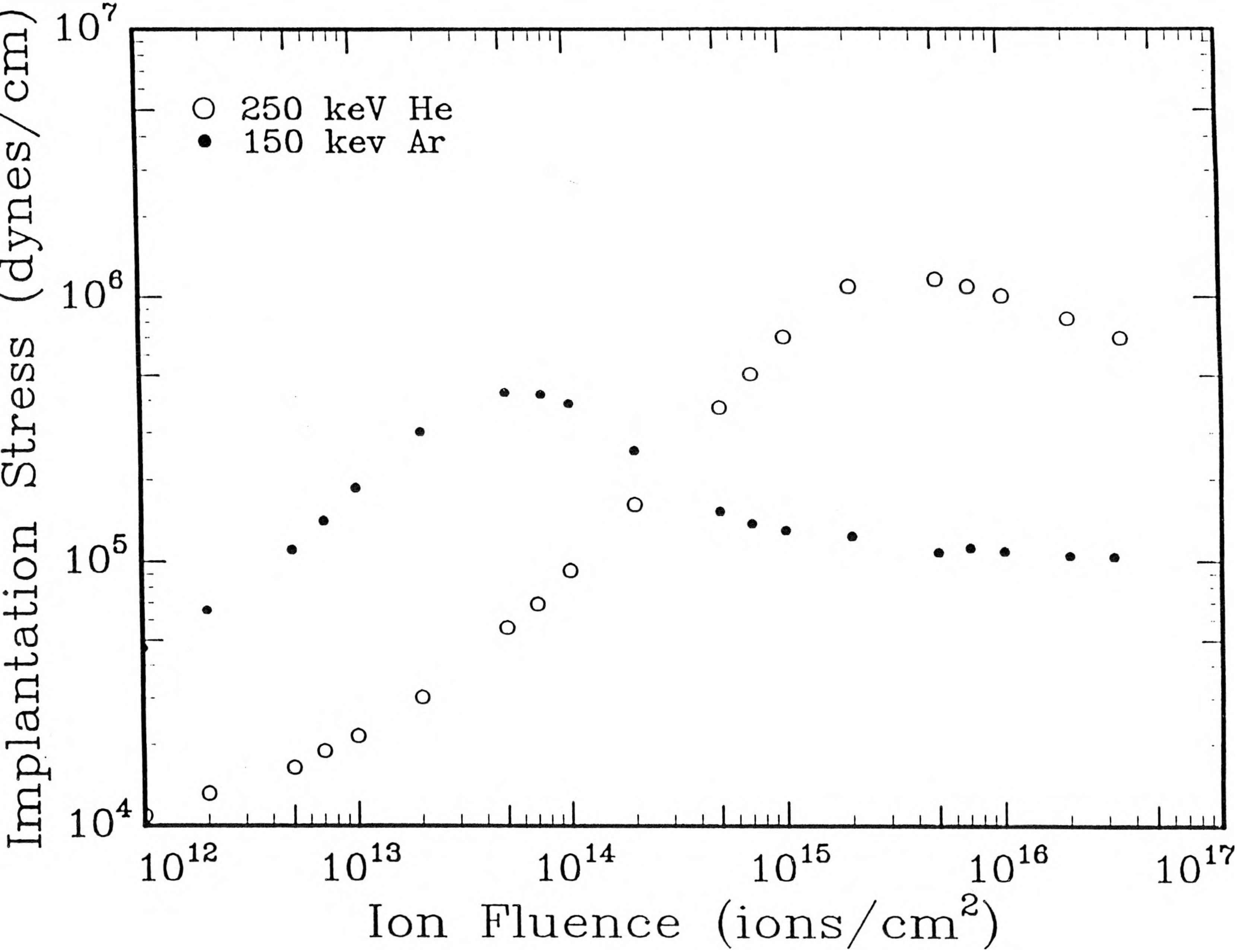

250 keV He
150 kev Ar
Implantation Stress (dynes/cm)
10^7
10^6
10^5
10^4
10^{12}
10^{13}
10^{14}
10^{15}
10^{16}
10^{17}
Ion Fluence (ions/cm^2)

Figure 3

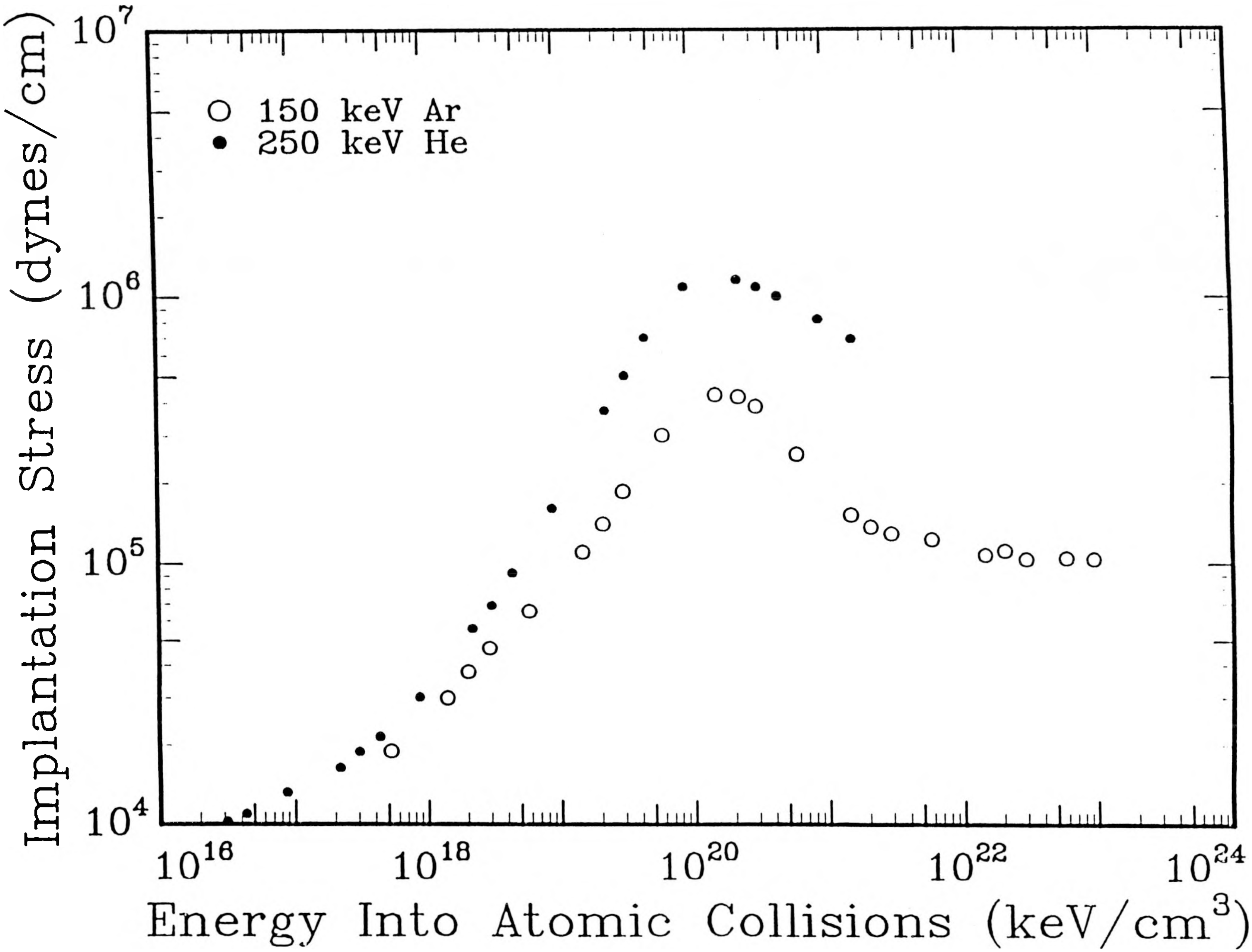
150 keV Ar
250 keV He
Implantation Stress (dynes/cm)
10^7
10^6
10^5
10^4
10^{16}
10^{18}
10^{20}
10^{22}
10^{24}
Energy Into Atomic Collisions (keV/cm^3)

Figure 4

Figure 5

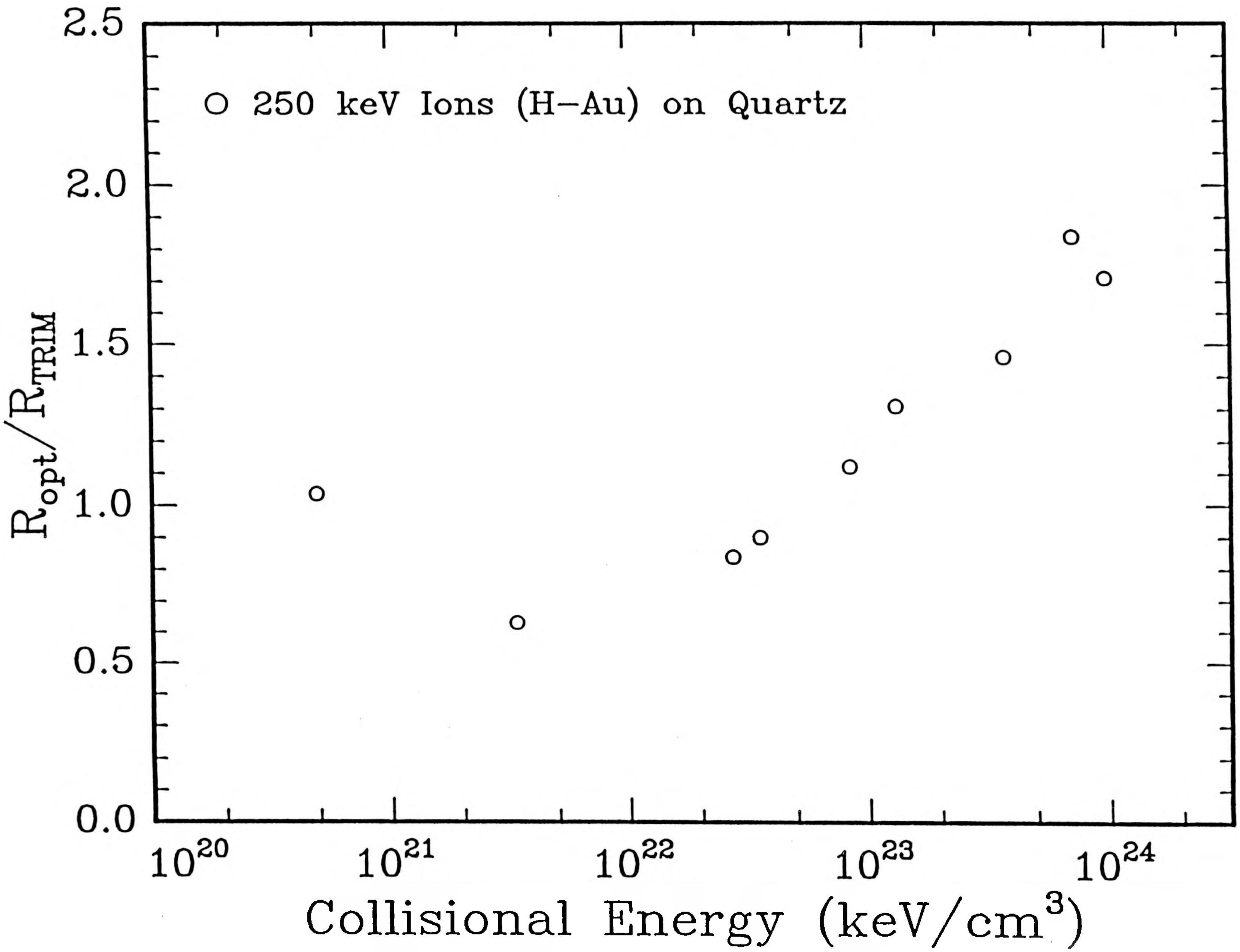

○ 250 keV Ions (H–Au) on Quartz
R_{opt}/R_{TRIM}
2.5
2.0
1.5
1.0
0.5
0.0
10^{20}
10^{21}
10^{22}
10^{23}
10^{24}
Collisional Energy (keV/cm^3)

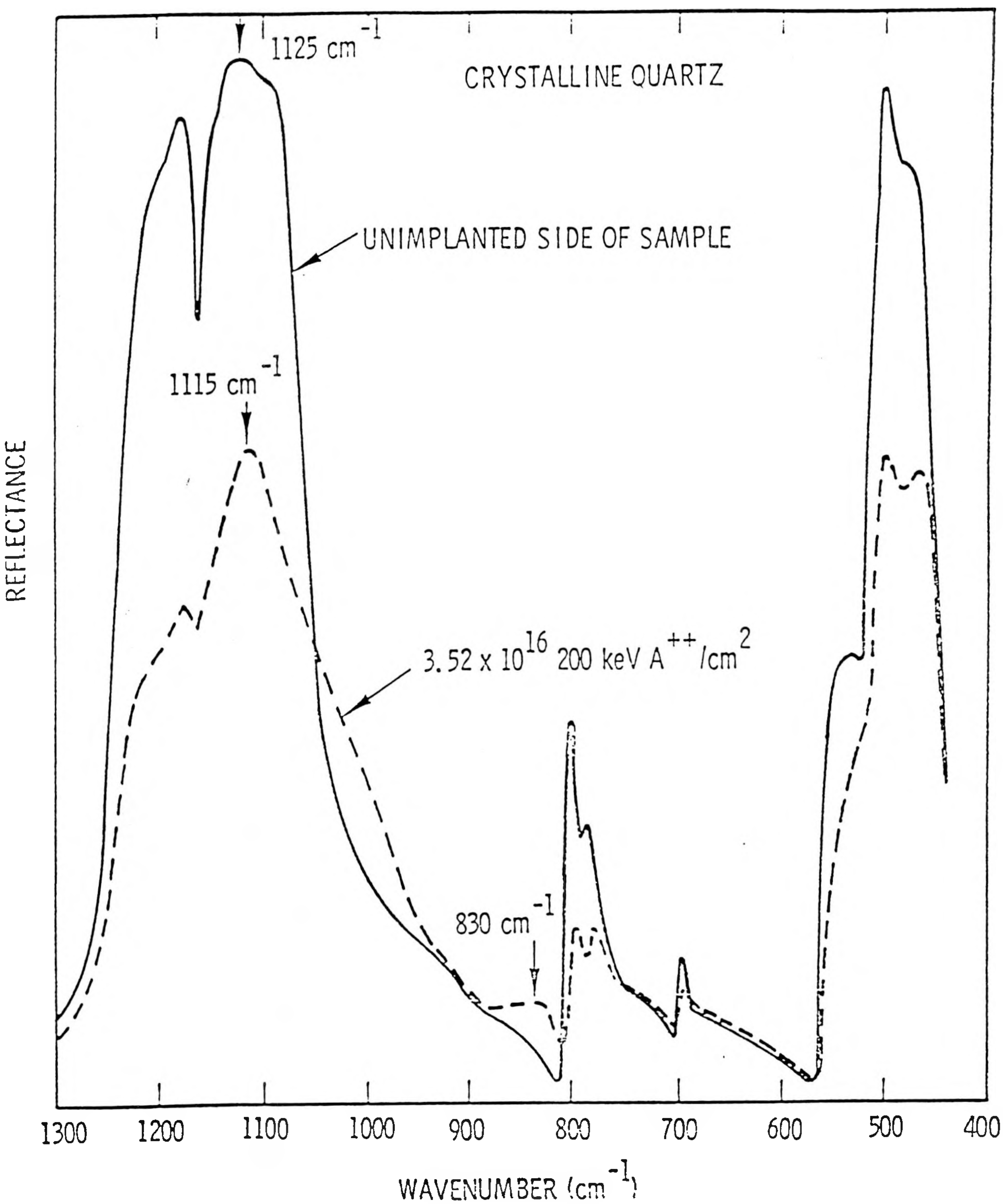
1125 cm-1
CRYSTALLINE QUARTZ
UNIMPLANTED SIDE OF SAMPLE
1115 cm-1
REFLECTANCE
3.52 x 10^16 200 keV A++/cm^2
830 cm-1
1300
1200
1100
1000
900
800
700
600
500
400
WAVENUMBER (cm-1)

Figure 6

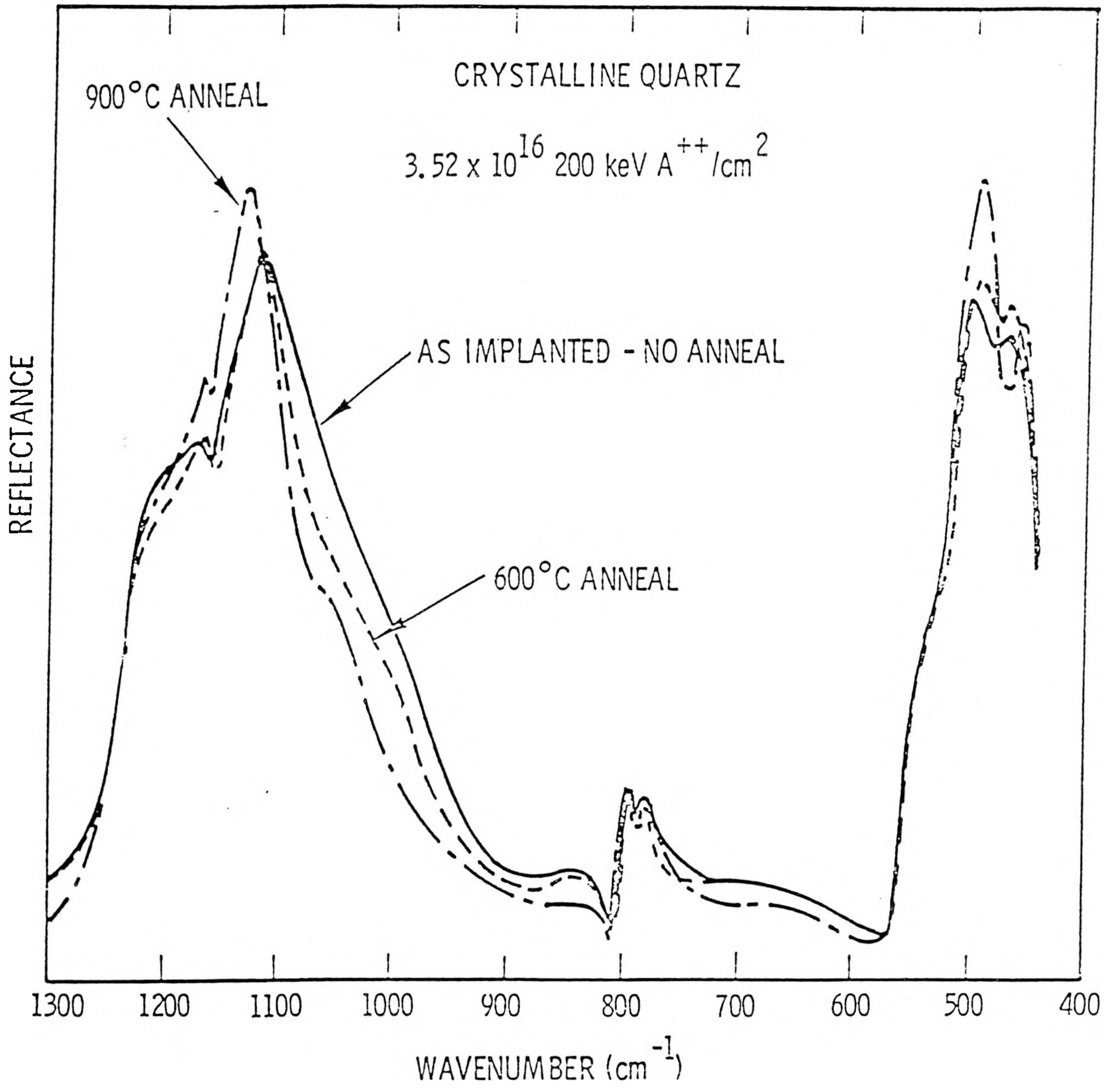

CRYSTALLINE QUARTZ
3.52 x 10^16 200 keV A^++/cm^2
900°C ANNEAL
AS IMPLANTED - NO ANNEAL
600°C ANNEAL
REFLECTANCE
1300
1200
1100
1000
900
800
700
600
500
400
WAVENUMBER (cm^-1)

Figure 7